J Mater Sci (2006) 41:7025–7032
DOI 10.1007/s10853-006-0024-9

Effect of powder treatment on the crystallization behaviour and phase evolution of Al_2O_3–High ZrO_2 nanocomposites

Raghunath P. Rana · Swadesh K. Pratihar · Santanu Bhattacharyya

Received: 28 February 2005 / Accepted: 19 September 2005 / Published online: 10 October 2006

Abstract Al_2O_3–ZrO_2 composites containing nominally equal volume fraction of Al_2O_3 and ZrO_2 have been synthesized through combined gel-precipitation technique. Subsequently the gels were subjected to three different post gel processing treatments like ultrasonication, ultrasonication followed by water washing and ultrasonication followed by alcohol washing. It was observed that while in unwashed samples crystallization took place at low temperature, crystallization was delayed in the washed gels. The phase transition of ZrO_2 in the calcined gels followed the sequence; amorphous → cubic ZrO_2 → tetragonal ZrO_2 → monoclinic ZrO_2. On the other hand, phase transition in alumina followed the sequence amorphous to γ-Al_2O_3, the transition taking place at 650 °C. No α-Al_2O_3 could be detected even after calcination at 950 °C. However, all the sintered samples had α-Al_2O_3. In spite of high linear shrinkage (19–21%) during sintering, the sintered sample had density of only above 70% for all the four varieties of the powders. However, in spite of the low sintered density of the pellets, 31% tetragonal zirconia could be retained after sintering at 1400 °C and it reduced to about 16% at 1600 °C.

R. P. Rana · S. K. Pratihar · S. Bhattacharyya (✉)
Department of Ceramic Engineering, National Institute of Technology, Rourkela 769 008, India
e-mail: santanub@nitrkl.ac.in

Introduction

The high elastic modulus of alumina makes it a suitable matrix to incorporate ZrO_2 particles for providing a tough ceramics. The increment in toughness mainly results from the transformation toughening and/or micro crack toughening effect [1, 2]. The enhancement in toughness is limited by the coarsening effect of ZrO_2 particles during sintering of the composites. A smaller intial particle size and a uniform distribution of fine ZrO_2 particles in tetragonal form is the desirable microstructure for toughened Al_2O_3–ZrO_2 composites [3, 4]. The extent of toughening achieved in these composites depends on size of Al_2O_3 and ZrO_2 particles, volume fraction of ZrO_2 retained in the tetragonal phase, which in turn will determine the volume fraction of tetragonal ZrO_2 available for transformation. A finer particle size distribution of ZrO_2 not only helps to achieve a uniform distribution of ZrO_2 particles, but it also ensures that ZrO_2 remains mostly in tetragonal phase provided the critical size barrier for the t-phase retention is not crossed [5]. Efforts to achieve a finer ZrO_2 and Al_2O_3 particle size have been made possible by use of sol–gel and other and process [6, 7]. However, in these studies the volume fraction of ZrO_2 particles was usually varied upto 30 vol% with very few reports on equal volume fraction of alumina and zirconia [8]. Higher volume fraction of ZrO_2 is expected to increase the fracture toughness of the composites due to higher volume fraction of tetragonal ZrO_2 available for stress-induced transformation. However, an increase in ZrO_2 volume fraction tends to cause inhomogeneous distribution of ZrO_2, higher grain size and consequently a lowering amount of retained tetragonal ZrO_2 content and low

fracture toughness. In our earlier study, we have reported the effect of calcination and sintering temperatures on the tetragonal phase retention on Al_2O_3–ZrO_2 composites prepared by gel precipitation route and containing nominally equal volume fraction of Al_2O_3 and ZrO_2 [9]. In the gel precipitation process, the viscosity of the starting mixed solution of $AlCl_3$ and $ZrOCl_2$ increases tremendously on addition of NH_4OH thus forming a network between precipitates. Thus during gelation process, while the precipitated mass becomes fully viscous; a substantial fraction of the starting solute still remains unreacted and remains entrapped in the gel network. On drying, these gels result in a hard fragile mass, which on calcination produces oxides via decomposition reactions. It was also observed in our previous study, that the fraction of retained tetragonal zirconia was quite low, being only about 20% at 1400 °C. Thus the aim of the paper is to study the effect of post-gelation powder treatment on the phase retention and densification behaviour of the composites. In the present investigation, although the samples were prepared by the same gel precipitation method, the gel was subjected to further processing like ultrasonication and ultrasonication followed by washing (in water as well as alcohol medium). The effects of this additional gel processing on the crystallization behaviour, phase evolution and densification behaviour have been systematically investigated in the present study.

Experimental procedure

The precursors were aluminum chloride ($AlCl_3$, AR grade) and zirconium oxychloride ($ZrOCl_2{\cdot}8H_2O$, AR grade). $AlCl_3$ and $ZrOCl_2$ were taken in a quantity so as to yield a nominally equal volume fraction of Al_2O_3 and ZrO_2. $AlCl_3$ solution of 0.5 moles per litre concentration was prepared in distilled water to which requisite amount of $ZrOCl_2$ was dissolved. To this clear mixed solution of chloride and oxy chloride NH_4OH was added in a drop wise manner while the solution was being vigorously stirred. Continued addition of NH_4OH resulted in the precipitation of hydroxides of Al and Zr along with an increase in the solution viscosity. Initially the viscosity increased slowly followed by rapid increase at a later stage. The addition of NH_4OH was carried out till the point at which the solution viscosity became so high that the stirring stopped automatically due to the viscous drag of the precipitated gel network. The pH at this stage was found to be between 6.5 and 6.7.

The gel was divided into four parts: one part which was dried as such was named as prepared (ASP) powder. Of the other three parts, one was subjected to ultrasonic treatment (USC powder), the other part was ultrasonicated followed by water washing (USW powder) and the last part was ultrasonicated and water washed followed by alcohol washing (USA powder). All the four varieties gels were dried at a temperature less than 100 °C and the dried gel was ground in an agate mortar and pestle. A small quantity of the dried gel was subjected to DSC/TG study (Netzsch 402 C) in an ambient atmosphere at a heating rate of 10 °C/min. The remaining portion of the gel of each type was calcined in air in the temperature range of 350 °C to 950 °C with a holding time of 9 h at the peak temperature. X-ray diffraction studies (Phillips PW-1830) were performed on the dried gels as well as calcined powders. The phase analysis was done by considering the standard XRD patterns of different polymorphs of alumina and zirconia. Crystallite size of the calcined powders was calculated from X-ray line broadening using Scherrer formula [10]. The densification behaviour of the calcined powders was studied on compacted cylindrical pellets. Cylindrical pellets (12.5 mm(ϕ, 3 mm high) were uniaxially compacted at 290 MPa. The calcined powder was mixed with 2 wt% PVA binder before compaction. The pellets were kept on a Pt disc and heated at a rate of 4 °C/min till 650 °C followed by heating at 3 °C/min up to the required temperature. The samples were sintered at 1400 °C, 1450 °C, 1500 °C, 1550 °C and 1600 °C. A hold time of 4 h was provided at each of the peak temperatures. Following the heating, the samples were cooled at 3 °C/min till 900 °C followed by furnace cooling. Bulk densities of the sintered samples were measured by Archimedes principle using kerosene as immersion liquid. The effect of washing on the type and nature of ions adsorbed on the gel powder surface was studied through FTIR. The spectra were taken in a diffuse reflectance (DRIFT) mode in a Shimadzu FTIR instrument (Model 84005). The gel powder sample was mixed with KBr and the spectra were taken in pellet form in the wave number range 4000–500 cm^{-1}.

Result and discussion

DSC/TG analysis

Figure 1(a–d) shows the DSC/TG curve for all the four types of gel powders viz. ASP, USC, USW and USA. Fig. 1a describes the DSC/TG behaviour of ASP gel.

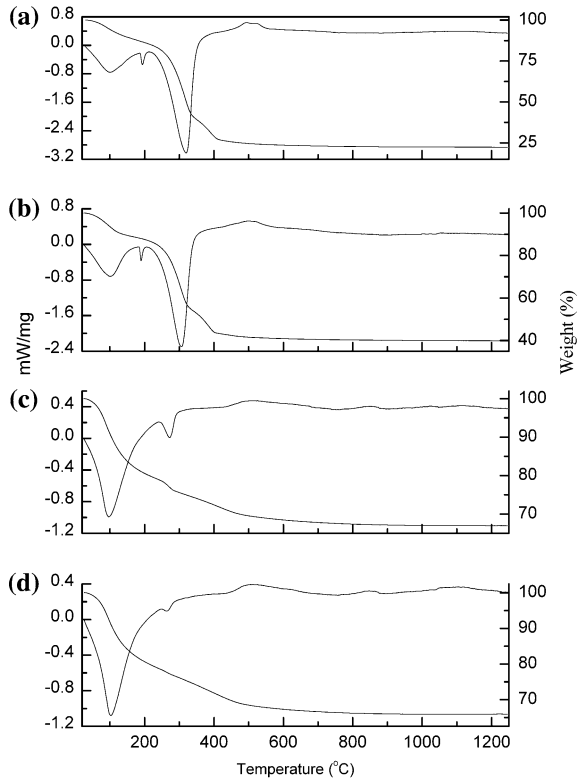

Fig. 1 DSC/TG of gel powders: (**a**) ASP, (**b**) USC, (**c**) USW and (**d**) USA

The curve has a broad endothermic peak at around 100 °C. This is associated with a gradual weight loss of 13.35% which continues till about 200 °C. The second endothermic peak at 194 °C is a sharp one without a corresponding weight loss in the TG curve. This peak therefore corresponds to reactions other than decomposition reactions. The third endothermic peak is of high intensity occurring at 320 °C. The associated weight loss is 48.4% and it continues up to 380 °C. The decomposition of NH_4Cl is a two-step process involving melting and sublimation. The standard value of melting and sublimation temperature is 220 °C and 338 °C, respectively. Since the melting does not involve weight loss, in the present study, it appears that the endothermic peak at 194 °C and the endothermic peak at 320 °C (associated with a weight loss of 48.4%) correspond to the melting and sublimation of NH_4Cl, respectively. The third stage of weight loss starts right after the second stage of weight loss and it continues till about 425 °C. The weight loss recorded in this stage is 12.27%. Immediately after the completion of weight loss two broad and shallow exothermic peaks are observed at about 490 °C and 500 °C. Following the two exothermic peaks, a small and gradual weight loss of 3.65% is observed till 1250 °C.

The probable chemical reaction associated with the combined gel precipitation process can be written as follows:

$$2AlCl_3 + 6NH_4OH = 2Al(OH)_3 + 6NH_4Cl \quad (1)$$

$$ZrOCl_2 + 2NH_3 + 3H_2O = Zr(OH)_4 + 2NH_4Cl + H_2O \quad (2)$$

$Al(OH)_3$ formed as per the Eq. (1) dehydrates in the temperature range 40–200 °C according to the reaction given below:

$$2Al(OH)_3 = Al_2O_3 + 3H_2O \quad (3)$$

The theoretical weight loss for this reaction is 34.6% and assuming Al_2O_3:ZrO_2::40:60(by weight), the weight loss should be around 13.8%. The observed weight loss is 13.65%, which is good agreement with the theoretical value. Following the similar logic, the theoretical weight for submilimation of NH_4Cl for the above sample will be 47.3%. The observed weight loss (48%) in the temperature range 250–350 °C thus matches well with the theoretical value and therefore the peak at temperature 320 °C corresponds to sublimation of NH_4Cl.

Subsequent to the decomposition of NH_4Cl, the DSC/TG curve shows a total weight loss of 15.85% occurring in two stages and two small and broad exothermic peaks in the temperature range 490–500 °C. The phases in ZrO_2 which develops on crystallization from an amorphous zirconium hydroxide ($Zr(OH)_4$ in this case) depends on the precipitation condition e.g. pH (high or low), fast or slow precipitation, etc [11]. It is also reported that large mass losses occurs till 1000 °C crystallization of Zirconia as $Zr(OH)_4$ do not crystallize directly to ZrO_2 but it goes through intermediate phases like $ZrO_{1.5}(OH)$ [11] according to the reactions

$$Zr(OH)_4 = ZrO_{1.5}(OH) + 1.5H_2O \quad (4)$$

$$ZrO_{1.5}(OH) = ZrO_2 + 0.5H_2O \quad (5)$$

The combined theoretical weight loss for Eqs. (4) and (5) is 15.6% which is good agreement with observed value of 15.8%. Thus, it can be concluded that $Zr(OH)_4$ forms on the reaction of $ZrOCl_2{\cdot}8H_2O$ with NH_4OH, crystallizes into ZrO_2 in two stages corresponding to the of two overlapping exothermic peaks in the temperature ranges 490–500 °C.

The above discussion was for as prepared (ASP) gel. The other three varieties of gel USC, USA, USW

(Fig. 1b–d) also show similar trends in weight loss during crystallization. However as washing of the gels removes most of the NH_4Cl from the gel, the weight loss in TG as well as decomposition peak (in DSC) for NH_4Cl are of lower magnitude/intensity for these gels. However, the DSC/TG plot of USC gel, Fig. 1b, shows that the two crystallization peaks have merged into a single peak at 505°C. Thus ultrasonication appears to have disturbed the gel structure resulting in simultaneous crystallization of Al_2O_3 and ZrO_2. Finally in the DSC/TG plot of USW and USA dried gels the two small and broad exothermic peaks are well separated i.e. at 520 °C and 850 °C. Thus, it appears that in the ASP and USC gel, the presence of the chloride ions lower the crystallization temperature and with washing the crystallization is delayed.

Phase analysis of dried gel powder

The XRD pattern of the dried gel powders is shown in Fig. 2(a–d). While Fig. 2a is the XRD pattern of the dried ASP gel powder, Fig. 2(b–d) is the XRD patterns of USC, USW and USA gel, powder, respectively. All the four patterns show that the dried gel powders are basically amorphous in nature. However, Fig. 2a and b contains some additional crystalline peaks, which are superimposed on the amorphous broad background. These crystalline peaks were identified to be of NH_4Cl, which forms due to the reaction of metal chlorides and NH_4OH. These additional peaks are absent in water washed as well as alcohol washed powders (Fig 2c and d, respectively). Thus washing removes NH_4Cl present in gel powder below that of the detection limit of XRD instrument.

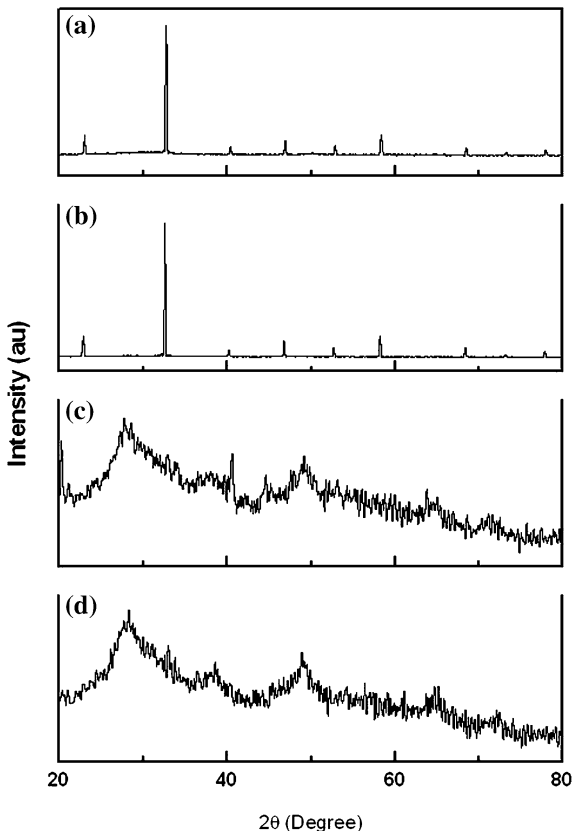

Fig. 2 XRD of gel powders: (**a**) ASP, (**b**) USC, (**c**) USW and (**d**) USA

Phase evolution in calcined powder

Figure 3(a–d) shows the X-ray diffraction pattern of four different types of calcined powders prepared in the method as mentioned before as a function of calcination temperature. It can be seen that ASP (Fig. 3a), USC (Fig. 3b) and USA (Fig. 3d) powder samples calcined at 450 °C show broad peaks, which could be identified to be cubic ZrO_2 (JCPDS File 81-1550). The broad nature of the peak indicates fine crystallite size of ZrO_2. The calculated crystallite size is 5.36 nm for ASP, 4.7 nm for USC and 5.36 nm for USA powder, respectively. USW (Fig. 3c) powder remained amorphous at 550 °C. Only at 650 °C, the USW powder shows crystalline peaks. The crystallite size for USW powder was 4.48 nm. All the four varieties of powder showed cubic ZrO_2 till 750 °C. At 850 °C, indications for the appearance of tetragonal ZrO_2 could be seen. The presence of t-ZrO_2 was identified on the basis of split peaks of (002) & (200) reflections. At still higher calcination temperature (i.e., 950 °C), a mixture of tetragonal and monoclinic ZrO_2 could be detected. The amount of retained tetragonal ZrO_2 at this temperature is 79%, 82%, 100% and 81% for ASP, USC, USW and USA powder, respectively. On the other hand, no crystalline phase of alumina could be detected till 550 °C. All the powders transformed to γ-Al_2O_3 at 650 °C, which persisted till 950 °C.

Table 1 shows the variation of crystallite for all the four types of powder calcined at different temperatures. It can be seen that at 550 °C crystallite size for USW powder is much smaller as compared to other three powders. This delayed crystallization along with smaller crystallite size for USW appears to be due to the combined effect of sonic energy and washing. This might have resulted in the formation of very fine crystallite size in the powder. Thus at lower calcination temperature, the diffraction peaks of USW powders were very broad and of low intensity thereby merging with the background. As the crystallite size increased on progressive calcinations at higher temperatures, the

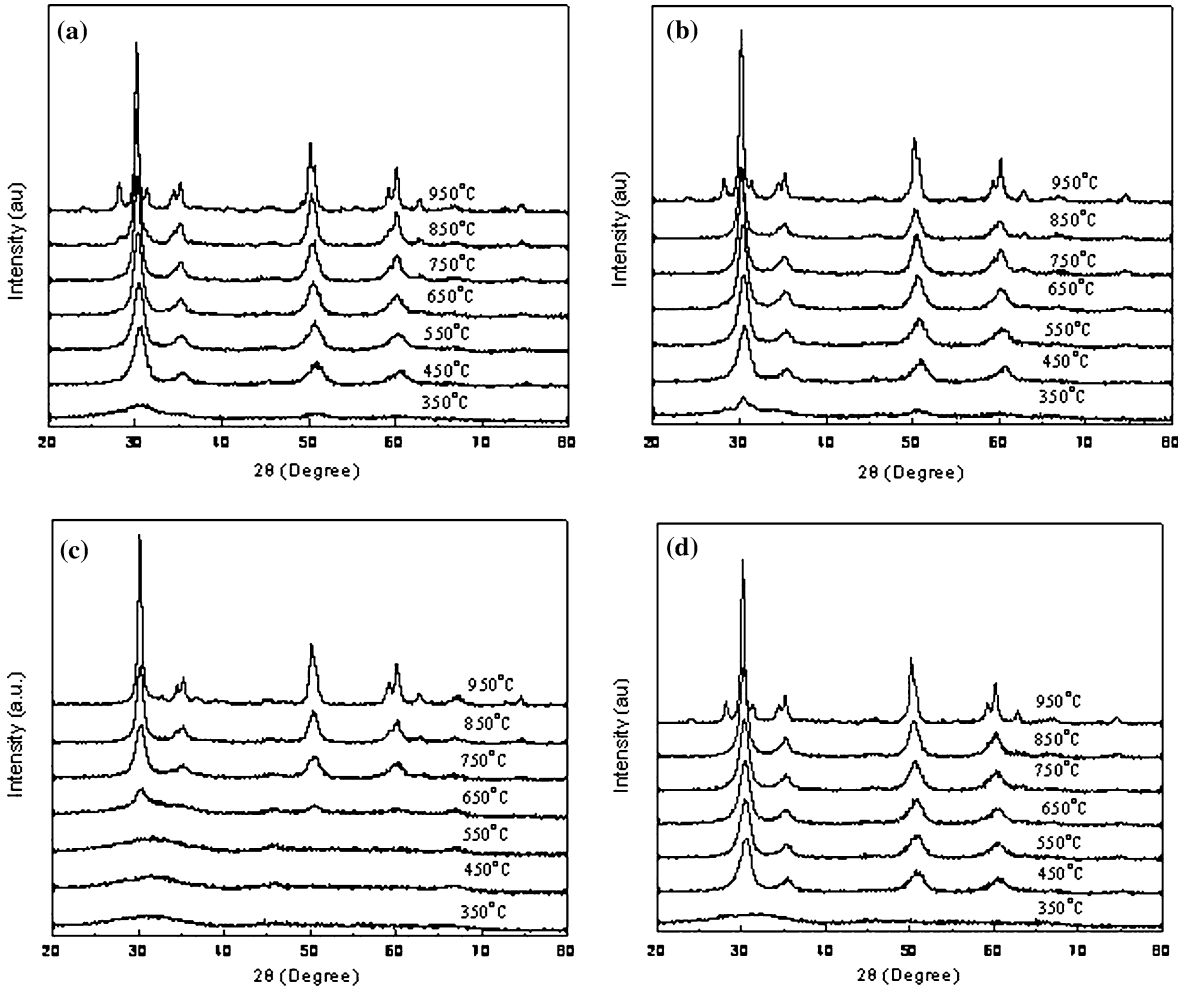

Fig. 3 XRD of calcined powder as a function of calcination temperature: (**a**) ASP, (**b**) USC, (**c**) USW and (**d**) USA

Table 1 Crystallite size as a function of calcination temperature

Temperature (°C)	Crystallite size (nm)			
	ASP	USC	USW	USA
450	5.36	4.7		5.37
550	5.98	4.83		5.51
650	7.35	4.87	4.48	6.15
750	9.14	5.06	4.95	6.37
850	12.43	6.3	6.04	8.3
950	18.689	12.59	11.05	17.28

peaks became sharper and stronger in intensity and it could be easily detected by the X-ray diffraction. However, it may be noted that due to high scattering factor of Zr^{4+}in comparison to Al^{3+}, in the lowered temperature calcined samples (viz. upto 550 °C), only ZrO_2 peaks could be detected and identified in the XRD patterns.

FTIR spectra

FTIR spectra of the four types of gel powder sample are shown in Fig. 4(a–d). The ASP gel powder (Fig. 4a) shows a broad peak from 3500 to 3000 cm^{-1} which could be assigned to the presence of $(OH)^-$ stretching vibration indicating the presence of structural water and adsorbed water. The peak around 2000 cm^{-1} corresponds to the hydrogen bonded OH group. The shoulder peak at around 2800–2750 cm^{-1} as well as around 1400 cm^{-1} corresponds to N–H bending from NH_3. The absorption peaks in the range 2300–2000 cm^{-1} corresponds to the combined stretching and bending vibration of OH groups of the hydroxides. The peaks near 1730 cm^{-1} correspond to the bending vibration of $(OH)^-$ group. The peaks in the range 1050–800 cm^{-1} are due Al–O vibration in the six coordinated Al ions. The absorption bands in the range 550–500 cm^{-1} are due to Zr–O vibration [12].

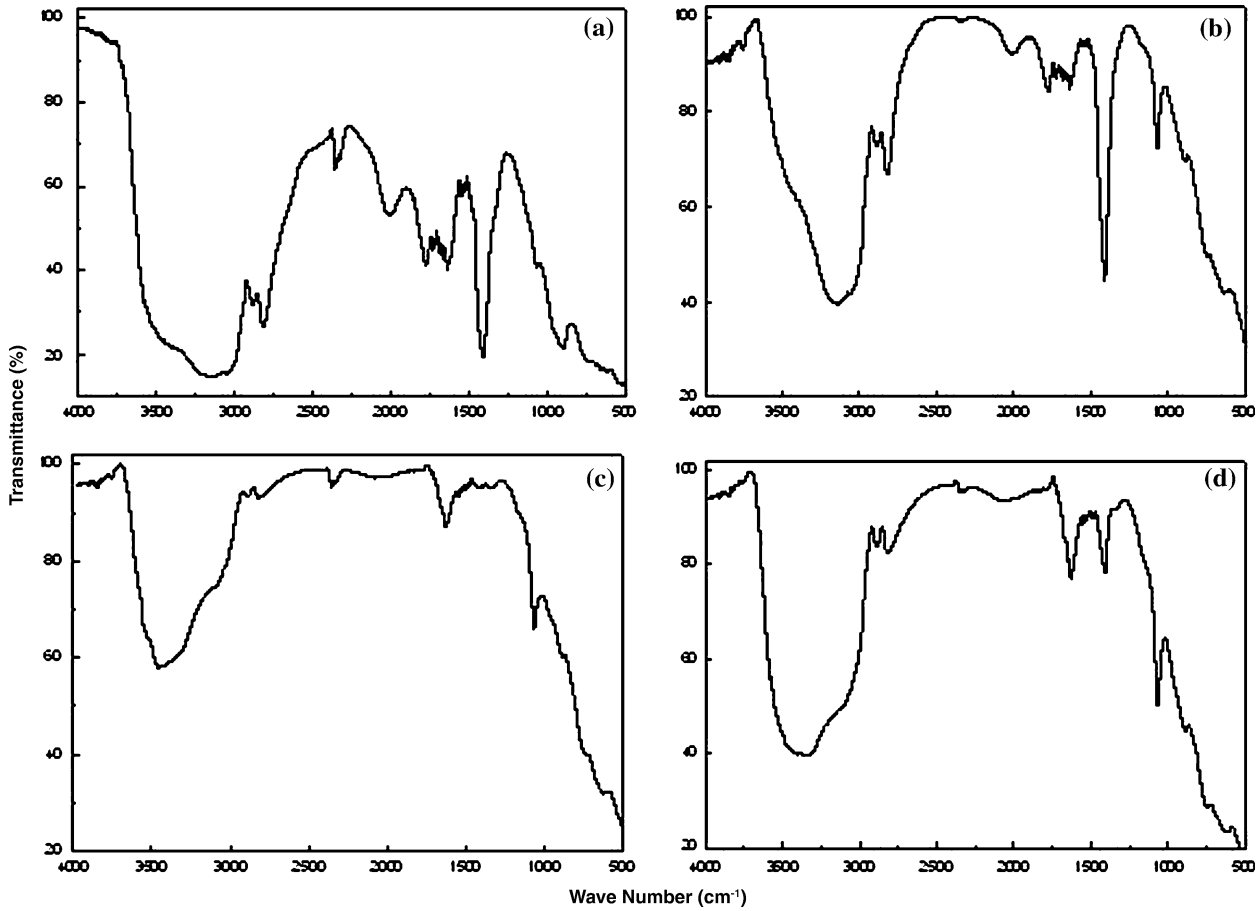

Fig. 4 FTIR spectra of gel powders: (**a**) ASP, (**b**) USC, (**c**) USW and (**d**) USA

Those peaks are diffused in ASP, USC gel powder and it increase in intensity in USW and USA powder.

The spectra of USC gel powder (Fig. 4b) has almost similar pattern and no extra peaks could be detected. Figure 4c shows the FTIR spectra of USW gel. It could be seen that the peak position are similar to that of ASP and USC gel but the peak intensities in the range 2800 and 1400 cm^{-1} are very small in comparison to the previous two spectra. This indicates that water washing partially removes the extra ammonia present. Thus the intensity of the peaks corresponding N–H groups decrease. Finally, Fig. 4d shows the FTIR Spectra of USA gel powder. The spectrum shows peak at 3500 cm^{-1} due to $(OH)^{-1}$ stretching from water and alcohol. The peaks due to N–H stretching and bending (in the wave number range 2800–2750 cm^{-1}) and has reduced very much. However, the spectrum also contains some extra peaks. The peak between 1600 and 1300 corresponds to C–O stretching from propanol and around 1000 cm^{-1} due to physical adsorbed propanol. Thus, different types of washing produce different kinds of adsorbed species on powder surface. Propanol washing removes extra $(OH)^{-}$ group and N–H groups. Thus these gel powders have relatively lower fraction of adsorbed $(OH)^{-}$ group from water. It is well documented that the presence of $(OH)^{-}$ group in the powder surface causes hard agglomerates due to hydrogen bonding during drying of these powders [13]. This result in poor densification of the compacts made from these powders. The absence of surface hydroxyl group from excess water is expected to produce soft agglomerates, which in turn are expected to produce improved sintered density for USA powder.

Phases in the sintered sample

The cylindrical pellets prepared from powder calcined at 850 °C for 9 h for all the four types of powder as mentioned before, were sintered in ambient atmosphere in the temperature range 1400 °C, 1450 °C, 1500 °C, 1550 °C and 1600 °C with a hold time of 4 h at the peak temperature. X-ray diffraction pattern of sintered pellets indicate that monoclinic ZrO_2 (d = 3.15 Å, JCPDS file: 83–0944) and α-Al_2O_3

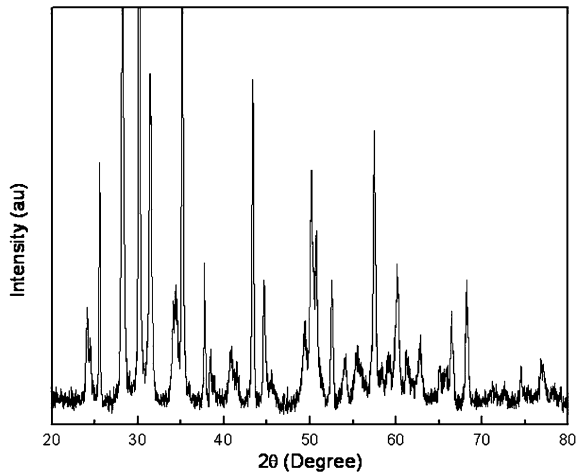

Fig. 5 XRD of ASP sample sintered at 1400 °C

(d = 2.09 Å, JCPDS file: 82–1467) were the major phase in the sintered sample. Besides monoclinic ZrO_2, the other ZrO_2 phase was tetragonal (d = 2.96 Å, JCPDS file: 81–1544). A representative XRD pattern of ASP sample sintered at 1400 °C is shown in Fig. 5a. The volume fraction of m-ZrO_2 and t-ZrO_2 were calculated using Schmid's formula [14] and the variation of t-ZrO_2 as a function of sintering temperature is Table 2. All the four type of samples show that the volume fraction of t-ZrO_2 decreases on increasing the sintering temperature. The decrease in retained t-ZrO_2 fraction results from an increase in the grain size of the sintered sample. However, in comparison to the other three samples the decrease is more gradual for USA sample and the fraction of retained t-ZrO_2 phase in this sample is also found highest. This could be related to alcohol washing effect of the gels which results in an initial smaller particle size and a comparatively smaller grain size in sintered sample, which facilitates higher retention of t-ZrO_2.

Densification behaviour of sintered pellets

Table 3 shows the sintered density of the four types of samples as a function of sintering temperature. The

Table 2 Tetragonal zirconia retention as a function of sintering temperature

Temperature (°C)	Retained t-ZrO_2 phase (volume %)			
	ASP	USC	USW	USA
1,400	38.75	33.87	32.85	37.24
1,450	29.36	19.41	29.46	22.28
1,500	21.21	13.06	22.16	21.79
1,550	19.89	9.7	18.8	16.86
1,600	9.66	6.72	14.16	7.26

Table 3 Sintered density of the samples as a function of temperature

Temperature (°C)	Sintered density (gm/cc)			
	ASP	USC	USW	USA
1,400	2.9	2.83	3.08	2.96
1,450	3.28	2.98	3.19	3.24
1,500	3.376	3.093	3.273	3.328
1,550	3.54	3.3	3.43	3.44
1,600	3.753	3.62	3.62	3.63

density data indicate that while sintered density increases with an increase in sintering temperature, the variation in the sintered density for the different type of samples is very insignificant. Thus at any particular temperature all the four type of samples had comparable sintered density. The linear diametral shrinkage of the samples was quite high and it varied between 19% and 21% for the samples studied. Thus inspite of very high shrinkage the sample showed poor sintered density (maximum sintered density 70% of theoretical). It was also observed that during sintering about 10% loss in weight was observed which is much higher than the anticipated weight loss from burning of PVA binder. Thus during sintering two processes occur simultaneously. One is shrinkage of the pellet causing densification and the other is creation of voids due to loss of materials. These two opposite action inhibit the density increase resulting in poor sintered density of the pellets.

Conclusions

Al_2O_3–ZrO_2 composites containing nominally equal volume fraction of alumina and zirconia have been processed through combined gel precipitation routes. Subsequently, the gel was subjected different treatment like ultrasonication of the gel, water washing and alcohol washing of the gel. It was observed that this post gel preparation treatments had effect on the crystallization behaviour and phase evolution of the calcined powder. While as prepared and ultrasonicated powder crystallizes at lower temperature (350 °C), washing delayed the crystallization. Washing of gels removes the NH_4Cl and excess NH_4OH present in the sample, which is revealed by X-ray diffraction and IR studies. Thus the difference in the crystallization behaviour could be attributed to the absence of NH_4Cl in the washed powders. Calcined powders from ultrasonicated gel had a lower crystallite size in comparison to other three varieties. It appears that the application of sonic energy causes the lowering in

crystallite size of the calcined powder. Sintered density of about 70% of the theoretical was obtained in all the four varieties of powder. Although the fraction of retained tetragonal was considerably higher (31%) in the samples sintered at 1400 °C, it reduced to 14% on sintering at 1600 °C. The lower retention of t-ZrO_2 could be attributed to lower sintered density. Studies are under way to increase the sintered density of the composites.

Acknowledgement This work is financially supported by Department of Science & Technology, Government of India.

References

1. Claussen N (1976) J Am Ceram Soc 59:49
2. Yuan LJ, Yen TS (1990) J Am Ceram Soc 75:2576
3. Novak S, Kosmac T, Ribitsch V (1995) Mat Sci Eng A 194:235
4. Freim J, Mckittrick J (1998) J Am Ceram Soc 81:1773
5. Srdic VV, Radonijc L (1997) J Am Ceram Soc 80:2056
6. Jayaseelan D, Nishikawa T, Awaji H, Gnanam FD (1998) Mat Sci Eng A 256:265
7. Prabhu GB, Bourell DL (1995) Nanostruct Mat 5:727
8. Balmer ML, Lange FF, Jayaraman V, Levi CG (1995) J Am Ceram Soc 78:489
9. Bhattacharyya S, Pratihar SK, Sinha RK, Behera RC, Ganguly RI (2002) Mat Lett 53:425
10. Cullity BD (1977) Elements of X-ray diffraction. Addison–Wesley Pub. Co. Inc., MA
11. Norman CJ, Goulding PA, Mcalpine I (1994) Catal Today 29:313
12. Saraswathi V, Rao GVN, Rama Rao GV (1987) J Mat Sci 22:2529
13. Kaliszewski MS, Heuer AH (1990) J Am Ceram Soc 73:1504
14. Schmid HK (1987) J Am Ceram Soc 70:367